Passive SAR imaging using the ASAR instrument of ENVISAT as transmitter of opportunity.

Virginie Kubica, Xavier Neyt
Royal Military Academy, Av. de la Renaissance 30, B-1000, Brussels, Belgium

Abstract

The ASAR instrument of ENVISAT can operate in Image Mode (stripmap-like mode) and in ScanSAR mode (burst mode) in which five sub-swaths are used to image large swaths at the expense of azimuth resolution. The poor azimuth resolution of the ScanSAR mode in monostatic configuration can be enhanced in the case of a bistatic configuration with a receiver close to the imaged area by using the sidelobe emissions of the beams illuminating the adjacent sub-swaths in addition to the mainlobe emissions of the beam illuminating the considered sub-swath.
In this paper, we describe the exploitation of the low azimuth resolution ScanSAR modes of the ASAR instrument and assess how the azimuth resolution can be improved from the nominal azimuth resolution based on real data acquired by a ground-based receiver.

1 Introduction

The ENVISAT Advanced Synthetic Aperture Radar (ASAR) provides various imaging modes from which opportunistic radars with receivers close to the imaged area can benefit thanks to their particular acquisition geometry. The Image Mode (IM) is used to produce high spatial resolution images over one of seven available swaths. The Wide Swath (WS) and the Global Monitoring (GM) modes use the ScanSAR mode with five sub-swaths to image large swaths at the expense of azimuth resolution due to shorter synthetic aperture length [1].
In monostatic SAR, the bursted nature of the ScanSAR signal creates discontinuities in the synthetic aperture. This yields a periodic modulation of the impulse response function which can be interpreted as the emergence of unwanted grating lobes. It is indeed shown [2, 3] that the point response in ScanSAR mode is a train of full-aperture (strip-map) point responses with the single-burst point response as envelope.
In opportunistic SAR, the sidelobe radiations of the beams illuminating the adjacent sub-swath and that fill the interburst intervals of the considered sub-swath can be exploited, thus allowing to increase the azimuth resolution while avoiding these grating lobes. Indeed, the bistatic nature of the radar is such that the transmitted signal is only attenuated by the one-way transmit-antenna pattern and the free-space loss transmitter-scatterer-receiver. However, the scatterer-receiver distance is much smaller than the scatterer-transmitter distance (monostatic case) leading to a smaller attenuation in the bistatic case.
Hence, for satellite passes exhibiting a favorable geometry, the ScanSAR mode can be exploited by an opportunistic SAR radar close to the imaged area to produce enhanced azimuth resolution images. As there are many more passes in ScanSAR mode than in Image mode, this results in a decreased revisit time over the considered area.
In this paper, we describe a method to enhance the azimuth resolution in ScanSAR mode by using the sidelobe emissions of successive ScanSAR beams. The achievable performance as a function of the scatterer position in the antenna beam is also analyzed.
The paper is organized as follows. Section 2 describes the considered passive bistatic radar. In Section 3, the azimuth resolution enhancement method is described and finally, Section 4 concludes the paper.

2 Passive SAR system

The bistatic imaging radar considered in this paper consists in an opportunistic spaceborne transmitter and a ground-based receiver operating in C-band (**Figure 1**).

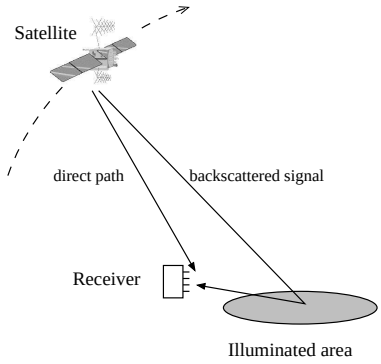

Figure 1: Geometry for the considered bistatic SAR

A backscattering geometry is considered to achieve the best possible range resolution [4, 5]. As an added benefit of this geometry, the direct signal from the satellite undergoes an additional attenuation as it is received via a sidelobe of the receiving antenna.

2.1 Reception system

Figure 2 shows the block diagram of the radar receiver which is extensively described in [6]. The receiver consists of a four-element uniform linear array antenna (an array of patch antennas) followed by four heterodyne receivers tailored for C-band. After amplification by LNAs (Low Noise Amplifier), the signals are analog down-converted to an intermediate frequency and then low-pass filtered to satisfy Nyquist-Shannon's sampling theorem. They are then sampled at 50 MSamples/s using a 16-bit A/D card (AlazarTech ATS660) and finally digitally down-converted to base-band.
Next, adaptive beamforming is performed to separate the reference signal (direct-path signal) and the reflected signal.
Finally, an image is synthesized from the separated signals using matched filtering.

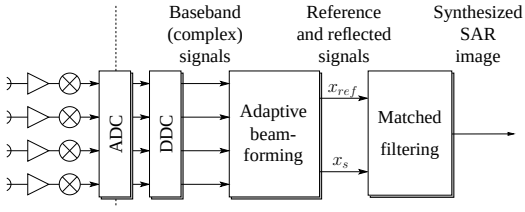

Figure 2: Signal Processing diagram with an analog (ADC) followed by a digital down-conversion (DDC)

2.2 Transmitter

The ASAR transmitter consists of an active phased array antenna of which the beams may be steered and shaped [1].

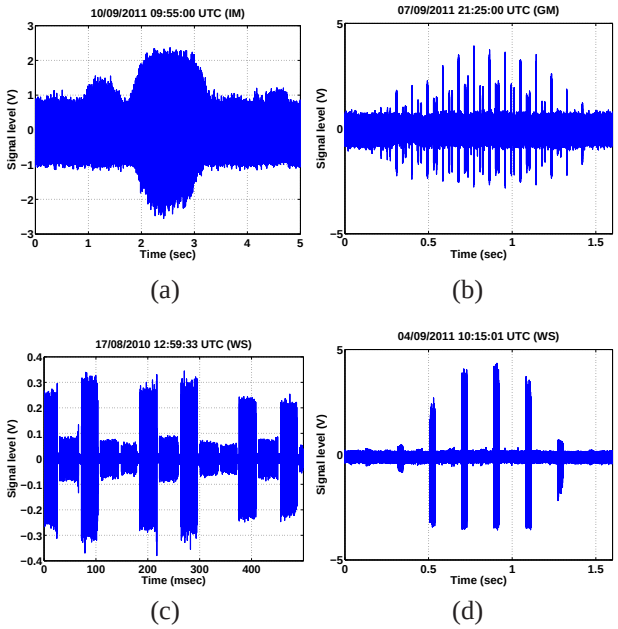

Figure 3: Examples of acquired signals (ENVISAT).

Typical received signals are depicted in **Figure 3**. The different modes of the ASAR instrument can be identified. The signal depicted in Figure 3 (a) results from an Image Mode (IM) transmission where pulses are sent at regular intervals. The azimuth antenna pattern of the transmit antenna can also be recognized. The signals in the other figures result from ScanSAR mode transmissions, where the transmit beam is steered in elevation to scan different part of the swath along track and in each beam, a burst of several pulses is transmitted. In the Global Monitoring (GM) mode (Figure 3 (b)), the bursts are shorter than in the Wide Swath (WS) mode (Figure 3 (d)) which corresponds to the announced smaller azimuth resolution. And indeed, as can be seen on Figures 3 (b) and (c), the bursts corresponding to different sub-swath are received. The amplitude of the bursts is obviously determined by the azimuth antenna diagram but also, for each beam, by the corresponding elevation antenna diagram at the elevation angle at which the receiver/scatterers are located.

3 Passive ScanSAR imaging

3.1 Signal model

Let us model the received signal as

$$y(t) = w(t)x(t) + n(t) \tag{1}$$

where $y(t)$ is the ScanSAR azimuth amplitude modulated signal with t the slow-time, $x(t)$ is the signal (pulses) transmitted by the transmitter assuming a constant amplitude (independent of the ScanSAR beam), $w(t)$ is an amplitude modulation function representing the transmitter antenna gain at the elevation of the receiver/imaged area and which varies with each ScanSAR beam and $n(t)$ represents the noise (thermal noise and eventual interference from scatterers located in the main beam). $x(t)$ and $n(t)$ are further assumed to be uncorrelated.

3.2 Peak-to-SideLobe Ratio

The impact of the ScanSAR mode on the image synthesis can be quantified using the Peak-to-SideLobe Ratio (PSLR) defined as the ratio of the peak intensity of the most intense sidelobe to the peak intensity in the mainlobe of the Impulse Response Function (IRF) along a one-dimensional profile (in the azimuth direction here).

$$PSLR_{dB} = 10\log_{10}\frac{\max(SL)}{ML} \tag{2}$$

where ML and $\max(SL)$ respectively stand for the mainlobe intensity and the maximum sidelobe intensity.

3.3 Matched filtering processing

In this section, the issues due to the ScanSAR mode and its countermeasure are illustrated using simulated data in the noise-free case. The basic parameters are those of a stripmap mode acquisition. A scenario with a point scatterer located far away from the range sidelobes of the

direct-path signal is considered in order to avoid direct path interferences on the scatterer impulse response. ScanSAR mode is simulated by the multiplication of the signal in the azimuth direction by a window, $w(t)$ as described in eq. (1). The length of the azimuth coherent processing determines the length of the window and the internal amplitude structure of the window represents the relative amplitude of the different beams in elevation as seen by the receiver/scatterers on the ground. This azimuthal amplitude modulation will vary with the position of the receiver/scatterer in the global swath (elevation angle) and is determinant as to the achievable azimuth resolution.

A single-beam ScanSAR mode, as would be obtained for a receiver/scatterer at the very edge of the wide swath illuminated by one single-beam would result in a pulse-train window modulation. The spectrum of that window predicts the azimuthal impulse response in the case of matched filter processing and as is well known [2, 3], grating lobes appear in this case, leading to a very poor PSLR of about -1dB.

When the receiver is favorably located, reception of signals from all five elevation beams is possible but each with a different amplitude according to the elevation antenna diagram of the considered beam. Processing of the data *as such* using matched filtering leads to a reduction of the amplitude of the grating lobes as shown in **Figure 4** (a) with a PSLR of -9.2dB, improved with respect to the PSLR of a single-beam ScanSAR.

3.4 Amplitude compensation

Further reduction of the PSLR can be obtained by adjusting the amplitude of the data in each burst by the proper azimuth gain correction function, commonly known as *descalloping window* [7] if $w(t)$ was an azimuth antenna pattern.

In order to cope with noise, this amplitude compensation is better recast as the problem of estimating $x(t)$ given the measurement $y(t)$. The estimation of the unknown transmitted signal, $x(t)$, can be done by designing the descalloping window $h(t)$ to minimize the Mean Square Error $E[|x(t) - h(t)y(t)|^2]$ between the desired signal $x(t)$ and its estimate, leading to

$$h_{opt}(t) = \frac{w(t)}{|w(t)|^2 + \frac{\sigma^2}{E[|x(t)|^2]}}, \qquad (3)$$

σ^2 being the variance of the noise.

Figures 4 (a) and (b) illustrate cuts along the point scatterer's isorange obtained respectively from ScanSAR data using a matched filter with and without compensation to correct for the ScanSAR-induced azimuthal amplitude modulation. For a SNR of $-10dB$, it should be remarked that the residual grating lobes due to the ScanSAR data totally disappear when $h_{opt}(t)$ is applied.

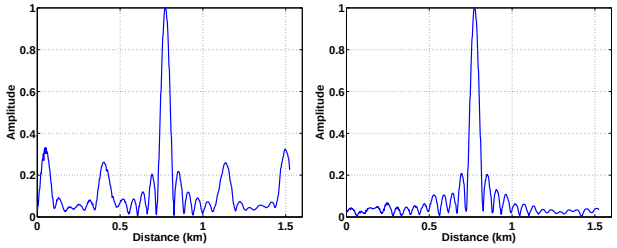

(a) (b)

Figure 4: Cut along the scatterer's isorange using the matched filter (a) without azimuth compensation (PSLR = -9.2dB) and (b) with azimuth compensation (PSLR = -12dB).

3.5 Performance assessment

The position of the receiver in the global swath is the paramount factor to assess whether or not the planned ScanSAR pass is suitable for amplitude-compensated azimuth resolution-enhanced SAR imaging. The bistatic geometry is calculated using the satellite position obtained with the help of an SGP4 orbit propagator and orbital information from the two line elements of ENVISAT. The position of the receiver is defined by its antenna elevation angle, i.e., the angle scatterer-transmitter-nadir.

For our bistatic application, the sidelobes of the elevation diagram are of utmost importance in order to predict the ScanSAR azimuthal amplitude modulation. As the European Space Agency (ESA) only provides the elevation antenna diagrams for 5° around the beam center, we used data acquired during six months to complement the elevation diagrams at other angles.

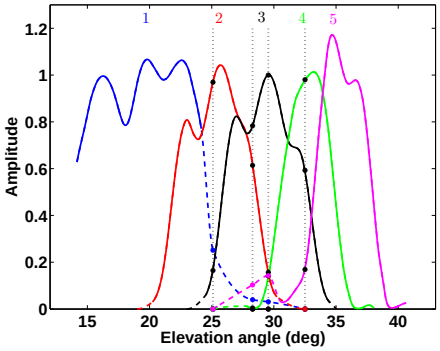

Figure 5: Extrapolated antenna elevation diagrams of the 5 beams. The colored dots denote our measurements and the black dots denote the values obtained from sampling antenna patterns provided by ESA.

Figure 5 depicts the ESA calibrated amplitude elevation diagrams of the five beams of ASAR used in ScanSAR mode (solid lines) and the extrapolation (dashed lines) based on our measurements.

Simulated satellite passes over $15^\circ \leq \theta_{el} \leq 40^\circ$ allow the computation of the PSLR of the IRF obtained with the conventional matched filter with and without compensation. **Figure 6** reveals that the PSLR of the matched filter

with compensation is by far better than without, at least for receivers/scatterer located in the elevation angle range $[27° - 32°]$.

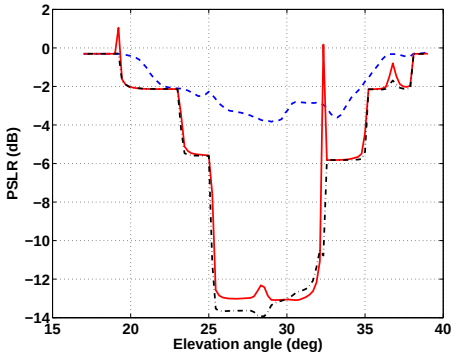

Figure 6: Calculated PSLR for different antenna elevation angles without compensation (dashed line), with compensation (solid line) and with compensation with increased regularization (dash-dotted line).

For the antenna elevation angles corresponding to a beam elevation gain close to zero (e.g. $19°$ or $32°$), the azimuth-compensated processing presents artifacts and is even less efficient than without compensation. Let us remind that the descalloping window $h_{opt}(t)$ was designed to minimize the MSE before azimuth focusing and not the PSLR. It turns out that the amplification due to $h_{opt}(t)$ is too excessive for a range of small values of $w(t)$. The net effect is that although the grating lobes are reduced, the noise is amplified leading to a larger PSLR. This excessive amplification can be controlled by introducing a parameter to increase the regularization in (3) that becomes

$$h_{opt,r}(t) = \frac{w(t)}{|w(t)|^2 + \alpha \frac{\sigma^2}{E[|x(t)|^2]}}, \qquad (4)$$

where α is the regularization parameter and is chosen equal to 100 for the increased regularization.
These low PSLRs reveal that an acceptable SAR image quality and thus an improvement of the azimuth resolution compared to the nominal ScanSAR processing can be expected. The PSLR is however not as small as in the monostatic case [8].
During these six months (June-Dec 2011), about 36 passes were recorded over Brussels of which 11 were false alarms. Out of the 25 remaining passes, 2 were in Image Mode while the other 23 were in ScanSAR mode (12 in GM and 11 in WS). The method can't be applied as such on GM overpasses since the interburst intervals are too large. And 7 of these 11 WS passes were in the favorable elevation angle range $[27° - 32°]$. This means that 64% had a PSLR low enough to guarantee an acceptable image quality.

4 Conclusion

In this paper, we propose an amplitude-compensated azimuth resolution-enhanced opportunistic SAR imaging for transmitters operating in ScanSAR mode. By exploiting signals received in the sidelobes of the elevation beams of the opportunistic transmitter, the poor announced azimuth resolution of the ScanSAR modes is increased. Beyond that, since ScanSAR passes occur more often than Image Mode passes, a decreased revisit time results.

References

[1] Y.-L. Desnos, C. Buck, J. Guijarro, J.-L. Suchail, R. Torres, and E. Attema, "ASAR-ENVISAT's advanced synthetic aperture radar," *ESA bulletin*, pp. 91 –100, May 2000.

[2] R. Bamler and M. Eineder, "ScanSAR processing using standard high precision SAR algorithms," *IEEE Transactions on Geoscience and Remote Sensing*, vol. 34, no. 1, pp. 212–218, 1996.

[3] J. Holzner and R. Bamler, "Burst-mode and scanSAR interferometry," *IEEE Transactions on Geoscience and Remote Sensing*, vol. 40, pp. 1917–1934, Sept. 2002.

[4] J. Sanz-Marcos, P. Lopez-Decker, J. J. Mallorqui, A. Aguasca, and P. Prats, "SABRINA: A SAR bistatic receiver for interferometric applications," *IEEE Geoscience and Remote Sensing Letters*, vol. 4, pp. 307–311, Apr. 2007.

[5] N. J. Willis and H. D. Griffiths, *Advances in Bistatic Radar*. Raleigh, NC: SciTech Publishing, 2007.

[6] E. Cristofani, V. Kubica, and X. Neyt, "A multibeam opportunistic SAR system," in *Proc. of the IEEE Radar conference*, (Kansas City, MI), May 2011.

[7] A. Monti Guarnieri, F. Rocca, P. Guccione, and C. Cafforio, "Optimal interferometric ScanSAR focusing," in *IEEE 1999 International Geoscience and Remote Sensing Symposium. IGARSS'99 (Cat. No.99CH36293)*, vol. 3, pp. 1718–1720, IEEE.

[8] B. R. Tell, P. J. Meadows, M. Tranfaglia, M. Santuari, A. Monti-Guarnieri, D. D'Aria, and I. N. Traver, "ASAR instrument performance and product quality evolution," in *2007 IEEE International Geoscience and Remote Sensing Symposium*, pp. 1401–1404, IEEE, 2007.